

Polarization dependent properties of waveguide arrays: band-structure anomaly and high-band localizations

Yoav Lahini, Daniel Mandelik and Yaron Silberberg

Department of Physics of Complex Systems, the Weizmann Institute of Science, Rehovot 76100, Israel
yoav.lahini@weizmann.ac.il

Roberto Morandotti

Institute National de la Recherche Scientifique, Varennes, Québec J3X 1S2, Canada

Abstract: We experimentally study polarization dependent linear and nonlinear dynamics in waveguide arrays. We found that in certain arrays, the band structure and the modal shapes of the array modes are markedly different for the two polarizations, in a manner that cannot be simply explained using the effective index approximation. Specifically, one of the gaps was found to be missing for the TM polarization. In the nonlinear regime, we observe mixed-polarization nonlinear localizations in high bands, such as Band-2 Floquet-Bloch vector solitons. The band structure anomaly enabled the excitation of a multiband moving breather.

©2005 Optical Society of America

OCIS codes: (190.4420) Nonlinear optics, transverse effects in; (130.2790) Guided waves; (190.3270) Kerr effect; (190.5530) Pulse propagation and solitons; 230.7370 Waveguides (230.4320) Nonlinear optical devices

References and links

1. D. N. Christodoulides, F. Lederer and Y. Silberberg, "Discretizing light behavior in linear and nonlinear waveguide lattices," *Nature* **424**, 817 (2003).
2. G. I. Stegeman and M. Segev, "Optical spatial solitons and their interactions: universality and diversity," *Science* **286**, 1518 (1999).
3. D. N. Christodoulides and R. I. Joseph, "Discrete self-focusing in nonlinear arrays of coupled waveguides," *Opt. Lett.* **13**, 794 (1988).
4. H.S. Eisenberg, Y. Silberberg, R. Morandotti, A.R. Boyd and J.S. Aitchison, "Discrete Spatial Optical Solitons in Waveguide Arrays," *Phys. Rev. Lett.* **81**, 3383 (1998).
5. D. Mandelik, H.S. Eisenberg, Y. Silberberg, R. Morandotti and J.S. Aitchison, "Band Structure of Waveguide Arrays and Excitation of Floquet-Bloch Solitons," *Phys. Rev. Lett.* **90**, 53902 (2003).
6. D. Mandelik, R. Morandotti, J.S. Aitchison and Y. Silberberg, "Gap solitons in waveguide arrays," *Phys. Rev. Lett.* **92**, 93904 (2004).
7. J. W. Fleischer, M. Segev, N. K. Efremidis, and D. N. Christodoulides, "Observation of two-dimensional discrete solitons in optically-induced nonlinear photonic lattices," *Nature* **422**, 147 (2003).
8. A. A. Sukhorukov, D. Neshev, W. Krolikowski, and Yu. S. Kivshar, "Nonlinear Bloch-wave interaction and Bragg scattering in optically induced lattices," *Phys. Rev. Lett.* **92**, 093901 (2004).
9. P. St. J. Russell, "Optics of Floquet-Bloch waves in dielectric gratings," *Appl. Phys. B* **39**, 231 (1986).
10. P. Yeh, A. Yariv, and C. S. Hong, "Electromagnetic propagation in periodic stratified media. I. General theory," *J. Opt. Soc. Am.* **67**, 423 (1977).
11. V.E. Zakharov, A.B. Shabat, "Exact theory of two-dimensional self-focusing and one-dimensional self-modulation of waves in nonlinear media," *Sov. Phys. JETP* **34**, 62 (1972).
12. S. V. Manakov, "On the theory of two-dimensional stationary self-focusing of electromagnetic waves," *Sov. Phys. JETP* **38**, 248 (1974).
13. J. U. Kang, G. I. Stegeman, J. S. Aitchison, and N. Ahkmediev, "Observation of Manakov soliton in AlGaAs planar waveguides," *Phys. Rev. Lett.* **76**, 3699 (1996).
14. A Villeneuve, J.U. Kang, J.S. Aitchison, and G.I. Stegeman, "Unity ratio of cross- to self-phase modulation in bulk AlGaAs and AlGaAs/GaAs multiple quantum well waveguides at half the band gap," *Appl. Phys. Lett.* **67**, 760 (1995).
15. J. S. Aitchison, D. C. Hutchings, J. U. Kang, G. I. Stegeman, and A. Villeneuve, "The nonlinear optical properties of AlGaAs at the half band gap," *IEEE J. Quantum Electron.* **33**, 341 (1997).

16. Z. Chen, M. Segev, T. Coskun and D. N. Christodoulides, "Observation of incoherently coupled photorefractive spatial soliton pairs," *Opt. Lett.* **21**, 1436 (1996)
17. D. N. Christodoulides, S. R. Singh, M. I. Carvalho and M. Segev, "Incoherently coupled soliton pairs in biased photorefractive crystals," *Appl. Phys. Lett.* **68**, 1763 (1996).
18. Jin U. Kang, G. I. Stegeman, and J. S. Aitchison, "Weak Beam Trapping by a Bright Spatial Soliton in AlGaAs Waveguides," *Opt. Lett.* **20**, 2069 (1995).
19. D. N. Christodoulides and R. I. Joseph "Vector solitons in birefringent nonlinear dispersive media," *Opt. Lett.* **13**, 53 (1988)
20. J. S. Aitchison, Jin. U. Kang, G. I. Stegeman, "Signal Gain due to a polarization coupling in an AlGaAs Channel Waveguide," *App. Phys. Lett.* **67**, 2456 (1995).
21. A. Schauer, I. V. Melnikov and J. S. Aitchison, "Collisions of orthogonally polarized spatial solitons in AlGaAs slab waveguides," *JOSA B* **21**, 57 (2004).
22. J. Meier, J. Hudock, D. Christodoulides, G. Stegeman, Y. Silberberg, R. Morandotti, and J. S. Aitchison, "Discrete Vector Solitons in Kerr Nonlinear Waveguide Arrays," *Phys. Rev. Lett.* **91**, 143907 (2003).
23. J. R. Salgueiro, A. A. Sukhorukov and Yu. S. Kivshar, "Spatial optical solitons supported by mutual focusing," *Opt. Lett.* **28**, 1457 (2003).
24. D. Mandelik, H. Eisenberg, Y. Silberberg, R. Morandotti and J.S. Aitchison "Observation of mutually trapped multiband optical breathers in waveguide arrays," *Phys. Rev. Lett.* **90**, 253902 (2003).
25. S. Flach and C. R. Willis, "Discrete Breathers," *Phys. Rep.* **295**, 181 (1998);
26. O. Cohen, T. Schwartz, J. E. Fleischer, M. Segev, and D. N. Christodoulides, "Multi-band vector lattice solitons," *Phys. Rev. Lett.* **91**, 113901 (2003).
27. A. A. Sukhorukov and Yu. S. Kivshar, "Multigap discrete vector solitons," *Phys. Rev. Lett.* **91**, 113902-4 (2003).

1. Introduction

1.1 Background

Light propagation in nonlinear periodic structures has been an active research area in recent years [1]. Early work on nonlinear propagation in continuous systems [2] has been extended to periodic structures, showing the similarities and uncovering the effects unique to a periodic nonlinear environment [3-8]. Optical waves propagating in a medium with spatially periodic refractive index distribution behave in a way that is analogous to electrons traveling through a semiconductor crystal, and their analysis often use terms like Brillouin zones, allowed and forbidden bands and other concepts borrowed from solid state theory. Nonlinearity, on the other hand, introduces a new element that has no analogue in electron physics, and combination of these two creates a diversity of new effects.

Arrays of evanescently-coupled waveguides provide a convenient platform for experimental investigation of periodic nonlinear systems in (1+1) dimensions. In particular, these arrays can model the dynamics of periodic nonlinear quantum systems where the transverse dimension represents a one-dimensional array of potential wells and the longitudinal (propagation) dimension represents the time evolution of standard quantum mechanics. Experimental realization of these arrays is particularly convenient in AlGaAs, which enables relatively easy design and manufacturing of refractive index patterns, and exhibits a significant Kerr nonlinearity.

Considering linear propagation in waveguide arrays, the dynamics can be divided into two broad cases. In the 'discrete' problem, much like in the tight binding model in solid state physics, the modes of each of the individual waveguides are evanescently coupled to each other, creating a band of allowed propagation constants. The gaps between the individual waveguide guided-modes become then the origin of the gap between these 'guided' bands. On the other hand, much like the nearly-free electron model in solid state physics, light beams for which the propagation constant lays beyond the set of guided propagation constants could be analyzed using Floquet-Bloch analysis, which can be formulated also in the optical domain [9,10]. Light propagation in this case resembles propagation in free 2D space with two distinct differences: first, the periodic potential imposes a periodic amplitude modulation on the beam. These are the Floquet - Bloch (FB) modal shapes, whose existence is postulated by the Floquet-Bloch theorem. Second, strong resonances between the light beam and the array

occur when the beam's K_x component (x being the direction perpendicular to the waveguides) is an integer multiple of the inverse of the lattice constant. At resonance all the reflected waves from the potential steps interfere constructively. As a result the beam is completely reflected from the array and a gap is opened in the allowed set of propagation constants, defining the 'antiguided' bands and gaps.

To analyze nonlinear propagation in these structures, theoretical and experimental work initially concentrated on the discrete problem, which was analyzed using the coupled mode theory [3,4]. In this formalism, the waveguides' bound states are evanescently coupled to each other, so when light is injected to one or a few waveguides in the array, it couples to adjacent waveguides as it propagates, thereby broadening its spatial distribution. In analogy to diffraction in continuous media, this process was termed discrete diffraction. When power is increased, the high light intensity changes the refractive index of the input waveguides through the Kerr effect and decouples them from the rest of the array. It has been shown that certain light distributions propagate while keeping a fixed spatial profile among a limited number of waveguides, forming discrete spatial solitons [3,4].

Recently, several studies went beyond the discrete model and investigated the band structure associated with the periodic waveguide array [5,6,8]. In particular, techniques were developed in order to inject light into a specific band [5]; Rather than injecting light directly into the waveguides, light was coupled at a grazing angle to the array, from an adjacent wide planar waveguide (i.e. the continuum) along the array's side (see inset of Fig. 2). By controlling the incidence angle, the beam's wave vector component along the waveguides direction, K_z , can be adjusted. This enables phase matched coupling to a particular value of β in the band diagram (see Fig. 1). The FB modal shapes were directly observed [5], and it was shown that each band has one specific FB mode associated with it. As the propagation constant is scanned, the transition from band to band is accompanied by a qualitative change in the modal shape of the beam, while within each band the modal shape is generally kept constant.

Figure 1 shows calculated band gap structure of a typical waveguide array, and measured band specific FB modal shapes (following [5]).

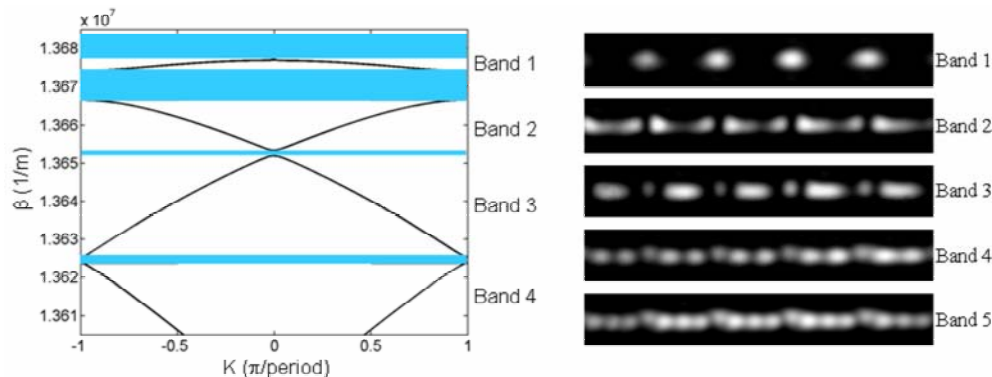


Fig. 1. Band gap structure of a waveguide array and measured Floquet–Bloch modes of each band: Calculated band gap structure for the waveguide array (left) reveals the allowed bands and the gaps. Light coupled to forbidden β is reflected back from the array, while light coupled to allowed β is coupled to a band specific Floquet–Bloch mode (right) (following ref. [5]).

Mandelik *et al.* have shown [5] that in the nonlinear regime, solitons can form at each band, exhibiting self-trapping while still keeping the unique FB modal shape of the band. These solitons were termed Floquet-Bloch Solitons. Close observation of the first band reveals that its modal shape is constructed from the waveguide guided modes, therefore the discrete solitons could be considered as FB Solitons of the first band.

The polarization properties of nonlinear guided waves have also been studied extensively in continuous systems. Vector solitons [11, 12] consist of two orthogonally polarized beams which are mutually trapped. In particular, a Manakov vector soliton exists when self-phase modulation (SPM) and cross-phase modulation (XPM) are equal, and the energy mixing term (FWM) vanishes; these vector solitons conserve power, linear momentum and soliton number (see ref [2]). Manakov spatial solitons were realized in an AlGaAs planar waveguide [13] using a beam with a frequency smaller than half the band gap of AlGaAs. In this case the nonlinearities for the TE and the TM polarizations are approximately equal, and the SPM to XPM ratio is close to unity [14, 15]. Other techniques to form non-beating coupled soliton pairs are based on incoherent beams [16,17]. AlGaAs slab waveguides have also been used to investigate possible trapping of a signal beam by a strong, orthogonal soliton [18], nonlinearly induced power exchange between polarization components [19,20], and collisions between orthogonally polarized solitons [21].

In this work we investigate the propagation and interaction of the two polarization components in both linear and nonlinear waveguide arrays. Recently, Meier *et al.* [21] studied the formation of discrete vector solitons in the first (guided) FB band. Here we study the polarization properties of higher (antiguide) bands. In the linear regime we focus primarily on an anomaly observed in certain arrays, where the band structure associated with the two primary polarizations showed marked differences. In the nonlinear regime, we explore self-phase and cross-phase modulation in various cases, and demonstrate basic self and mutual trapping phenomena. Finally, we use the linear anomaly to excite a novel composite excitation.

1.2 Experimental setup

The laser source was a commercial optical parametric oscillator (Spectra-Physics *OPAL*), pumped by a 810nm Ti:Sapphire (*Tsunami*) laser, producing 4nJ pulses at a repetition rate of 80MHz. The average power is 320mW, the pulse peak power is about 40kW, the pulse length is about 120fsec and the wavelength is 1530nm. We use this wavelength in order to achieve optimal nonlinear response of our AlGaAs samples, in terms of the Kerr-coefficient to nonlinear-absorption ratio [15].

A schematic drawing of the sample used in our experiments is shown in the inset of Fig. 2. The array is made from a slab of AlGaAs planar waveguide composed of three layers: an 18%, 1.5 μ m thick, aluminum mole-fraction core, sandwiched between two cladding layers of 24% aluminum mole-fraction on top of a GaAs substrate. The upper and lower claddings were 1.5 μ m and 4 μ m thick, respectively. The waveguides are patterned onto the slab waveguide by means of conventional photolithography techniques, followed by plasma etching. The etched area of the slab has a lower effective refractive index, and using the proper mask, a set of one-dimensional linear waveguides is formed. The array period was 11 μ m, and the lateral effective refractive-index step was 0.007. We choose to work with 4 μ m-wide waveguides that support a single guided mode. The Kerr coefficient for TE and TM polarizations in such waveguides were previously measured to be $n_2 = 1.5 \times 10^{-13}$ and 1.43×10^{-13} cm²/Watt, respectively. The linear birefringence is estimated to be of the order of 10^{-4} [13, 22].

The experimental setup is shown in Fig. 2. The input power is tuned using a variable attenuator, and an elliptical beam shape with the desired width is obtained using cylindrical optics. A half Waveplate is used to control the beam's linear polarization direction. The light is coupled into the sample using an X40 objective lens. A 1mm thick glass window is inserted in front of the input objective lens. Rotation of this window results in small translations of the beam, which are transformed by the objective lens into small beam tilts at the sample input facet. As explained earlier, this enables us to effectively control the propagation constant β of the excited FB-mode in the array. In this geometry the beams travel a very short distance in the slab waveguide before entering the array, therefore no significant nonlinear effects are expected to take place there. At the most, slight focusing of the beam could result in a slight broadening of the beam's spectrum on the β axis. After propagating along the sample, light is collected from the output facet by a second objective lens. A beam splitter is used to sample

output power, given throughout this paper in terms of peak power. The output objective lens images the light from the output facet onto an IR sensitive camera. Finally, a top view of the array is imaged onto a CCD camera. This camera is used to monitor the beam propagation in the sample by collecting multiphoton fluorescence at the AlGaAs band gap (740nm) excited by the high-power beam, mainly through three-photon absorption [24]. This fluorescence enables a unique view of the beam along its propagation direction.

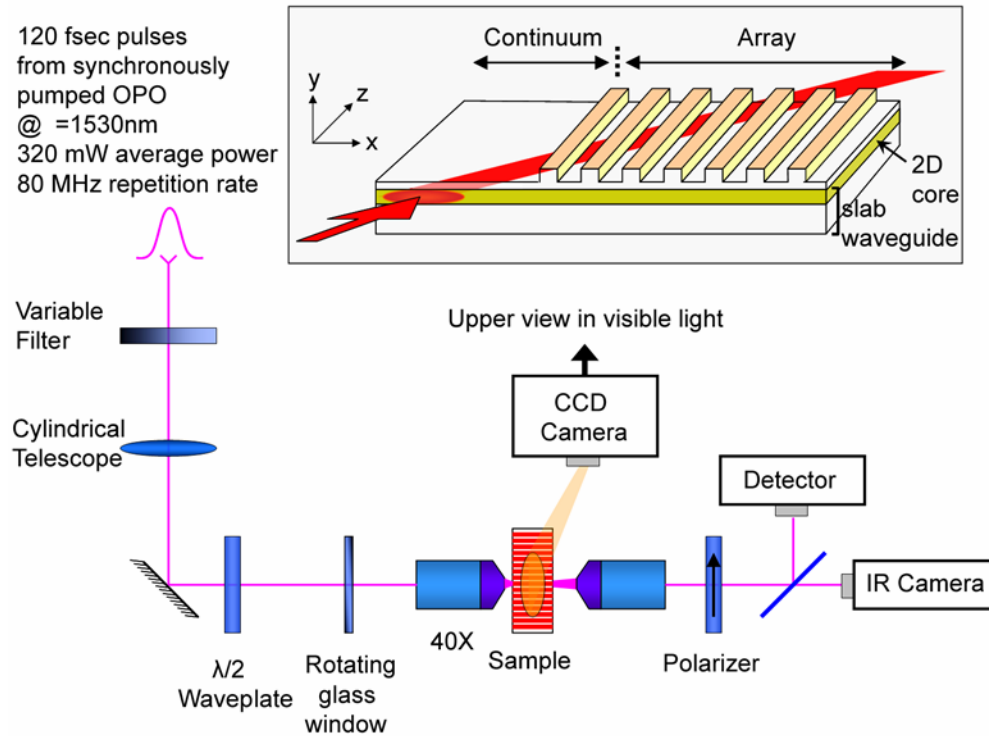


Fig. 2. The experimental setup. Inset: schematic drawing of the sample and the light coupling geometry

2. Linear band structure and Floquet-Bloch modes for the TE and TM polarizations:

We studied the band structure of the array described above. In order to excite a single FB mode in the waveguide array, we couple a beam at a grazing angle to the array, from a region of a wide planar waveguide (i.e., the continuum) along the array's side (see inset of Fig. 2), [5]. A wide input beam (about $70\mu\text{m}$ FWHM) was used, defining a narrow spectral content of the excitation. By scanning the input beam's angle we explore the band gap structure of the array. For angles matching the band gaps the beam is almost totally reflected from the array's interface, back into the continuum region. Between the gaps, the beam excites pure FB modes.

Figure 3 shows cross sections of the beam at the sample output plotted as a function of the input beam angle, for both the TE (a) and the TM (b) polarizations. Our setup enables light coupling to bands 2 to 5. We could not observe band 1 in this coupling scheme since the range of available propagation constants was limited (from above) by the etched continuum (see [5]).

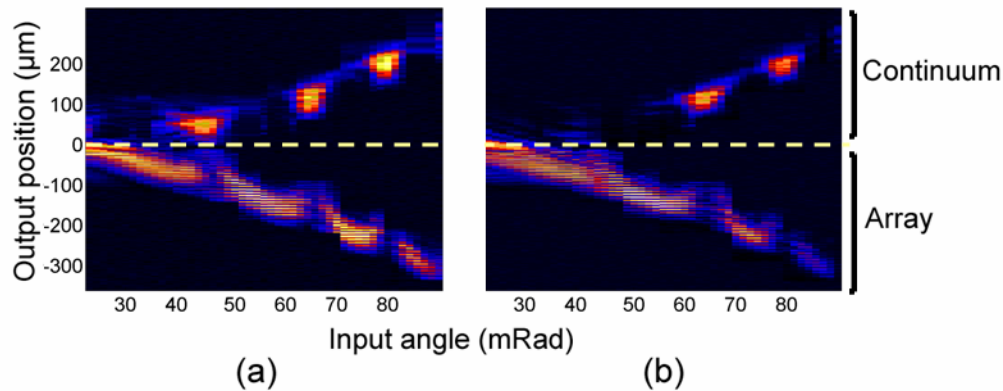


Fig. 3. Measured band gap structure of a waveguide array in TE and TM polarizations: Cross sections of the measured intensity distribution at the sample output as a function of the input beam angle for (a) TE polarization and (b) TM polarization. For angles that match the band gaps the beam is reflected from the array interface, back into the continuum region. Between the gaps, the beam excites pure FB modes. For the TM polarization the gap between band 2 and band 3 is missing.

These results show the anomaly in the gap between band 2 and band 3; the gap is very clearly seen in the TE data, while it is almost totally absent in the TM case. An experiment with an even a wider beam (allowing higher spectral resolution) failed to recover the missing gap. For the TM case, the transition between bands 2 and 3 seems continuous. This is better exemplified by a magnified view of the output intensity distribution at these angles – see Fig. 4 (Video). The evolution of the modal shape of band 2 into the modal shape of band 3 is smoother for the TM field, while for TE field there is a significant reduction in the transmission intensity at the transition angle due to the gap reflection.

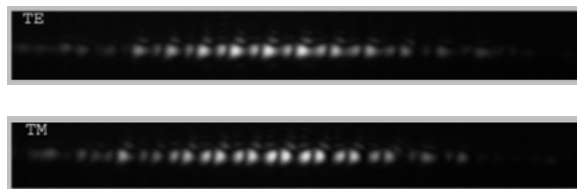


Fig. 4. Band 2 to Band 3 transition in TE and TM (movies): These movies show a magnified image of the beam at the array output, with input beam angle scanned around the transition between bands 2 and 3 for TE (top) and TM (bottom) polarization. The characteristic modal shapes for bands 2 and 3 are clearly observed. In the TE polarization there is a significant reduction in the transmission intensity at angles corresponding to the transition between bands 2 and 3 due to the gap reflection, and the transition seems discontinuous. In the TM polarization the transition is smoother – the reduction of transmitted intensity in the transition angles caused by the gap reflection seems to be much lower, and the evolution of the 2nd band modal shape into the 3rd is smooth and clearly seen.

We also found that the transition between the band 2 and band 3 occurs at smaller angles in the TM polarization. Consequently there is a well defined range of input-beam angles, in which launching a mixed polarization beam results in a unique situation in which the TE component is coupled to band 2, while the TM component is coupled to band 3, as seen in Fig. 5.

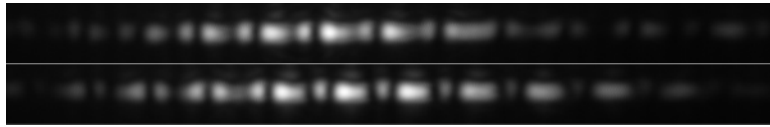


Fig. 5. Photographs taken at the array output, for a mixed input beam at an angle of 43 mrad, in which the TE component (top panel) is coupled mainly the second band, while the TM component (bottom panel) is coupled mostly the third, as can be clearly seen from the different modal shapes.

Another interesting observation is shown in Fig. 6. The TM modal shape for the second band is markedly different than that of the TE mode, being expressed in smaller intensity occupying the region between the waveguides.

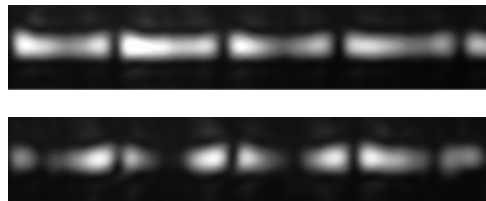


Fig. 6. Different TE and TM modal shapes in the second band: A magnified view showing the different modal shapes of the second band for TE (top) and TM (bottom) polarizations.

We note that all other observable bands and gaps (bands 3-5), did not exhibit such differences; the two polarization states seem to have practically identical modal shapes; the gaps reside at the same angles and have similar widths. We also note that other arrays with different periodicities and index-steps also exhibited polarization related differences, yet the most pronounced anomaly was found in arrays identical to the one described above.

The widely-used effective-index approximation (reducing the two-dimensional modal problem into a product of two one-dimensional problems) which has been used for calculating the band gap structure of waveguide arrays, failed to predict these observations. Separate calculations were conducted for each polarization, using the known birefringence of a slab waveguide and taking into account the different boundary conditions [10]. These calculations yielded no apparent differences in the band gap structure. In addition, our numerical calculations failed to predict any waveguide-induced birefringence for these samples. Apparently, a full two-dimensional vectorial calculation is required in order to understand these results. These unexpected polarization dependent properties may prove to be an important design consideration for waveguide arrays.

3. Nonlinear localizations

In all the following experiments we used a narrow beam (about 35 μ m FWHM) to achieve higher light density and to enhance diffraction, and examined the results of increasing the beam's power on its propagation in different cases.

3.1 Formation of TE and TM Floquet-Bloch solitons

It has been demonstrated [5] that at high powers it is possible to form FB solitons – self trapped beams that maintain the characteristic modal shape associated with each of the bands. We have verified that we can generate such solitons both for TE and TM waves (Fig. 7). Here, too, the nonlinear FB waves maintain their linear modal shapes. In particular, the modal shape of the FB-soliton of band 2 looks different when measured in TM and TE polarizations, as in

the linear case described above. We observed that also at high powers, the band structure lacks the gap between band 2 and band 3 for the TM polarization (not shown).

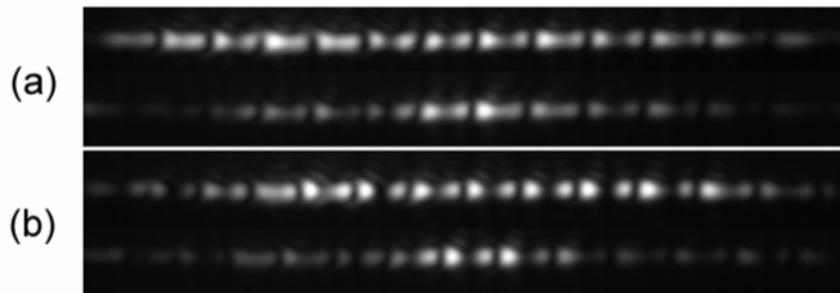


Fig. 7. Formation of Floquet-Bloch solitons for TE (a) and TM (b) beams (top – low power, bottom – high power), coupled to band 2. Both polarizations exhibit self focusing and soliton formation, while keeping their characteristic modal shapes, being different for TE and TM polarizations, as in the linear case.

3.2 Mixed-polarization nonlinear localizations in high-bands

In the following experiments, the waveplate was adjusted so that the input beam is composed of *both* TE and TM components. It is well known that there are two important limits when a field which contains both polarization component propagates in a nonlinear medium [13,20-22]. When the birefringence is large compared with the induced nonlinearity the two components interact incoherently. Yet, when the nonlinearity could balance the birefringence, they interact coherently, and may exchange power. Thus, we experimentally checked for power exchange between the TE and TM components at high powers for a linearly polarized input beam at various polarization angles. In particular, for a mixed linearly polarized beam with a strong TM and a weak TE components, the power in the weak TE beam changed by less than 10%. We conclude that we are working in a regime in which the TE and TM components could be effectively treated as two mutually incoherent beams.

3.2.1 Excitation of vector Floquet – Bloch Solitons

We begin with the case of TE and TM components carrying equal power. Recently Meier *et al.* [22] have experimentally demonstrated formation of *discrete* vector solitons in AlGaAs waveguide arrays. At sufficiently high power levels the beam locked into a highly localized vector discrete soliton that required the presence of both polarization components of the beam. In this section, we demonstrate experimentally the existence of *Floquet-Bloch vector solitons*; That is, we show self-trapping of the composite beam in higher, antiguided bands of the band structure. We verify that the trapping occurs only when both components are present. When only one of the two is present, it lacks the power needed for self-trapping, and exhibits strong diffraction.

To excite a Band-2 FB vector soliton, a mixed beam, with nearly equal amounts of TE and TM polarizations is launched into the array in the side-coupling geometry, such that a pure Band-2 FB mode is excited in the array. The experimental results are shown in Fig. 8, presenting the light distribution at the sample output of the different components at different power levels. At low power (linear propagation) the input beam diffracts strongly. At high power, the beam focuses to its initial (i.e. input) width, implying that a Band-2 FB vector-soliton has formed. When launching each component separately into the array, at a power which equals that of the corresponding component constituting the mixed beam (i.e. half of overall beam power), the TE and TM components diffract almost as in the linear case, as can

be seen by comparing with the low power pictures of the two components. This proves that indeed, a *jointly-trapped* vector soliton has been excited in the array.

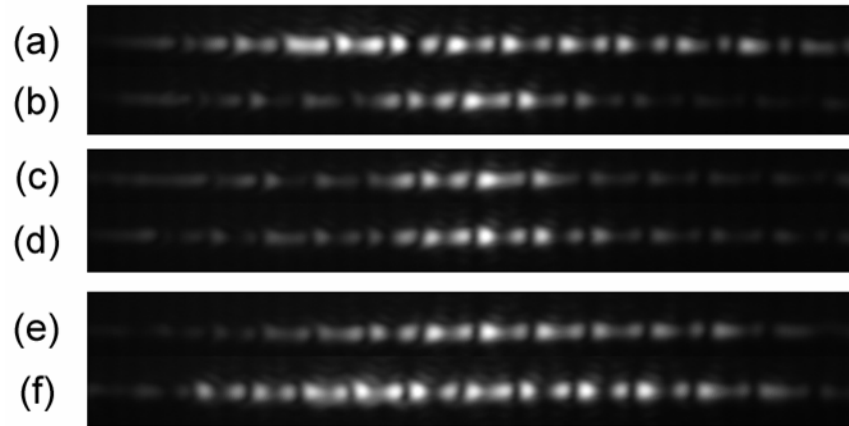


Fig. 8. Formation of a band-2 FB vector solitons: A beam with nearly equal TE and TM components was launched into the waveguide array in a side coupling geometry, such that a pure band-2 is excited in the array, as can be clearly seen from the characteristic modal shape. (a) At low power the mixed input beam diffracts strongly. (b) At high peak power of 1100 W the beam focuses to its input width, implying that a band-2 FB vector soliton has formed. At this state, the beam constitutes a TE component with a peak power of 540 W (c) and a TM component with a peak power of 560 W (d). When launching each component separately into the array, at a power which equals that of the corresponding component constituting the mixed beam, the TE (e) and TM (f) components do not localize (although focusing somewhat). This proves that indeed, a jointly-trapped vector soliton has been excited in the array.

3.2.2 Guiding of a weak Floquet-Bloch mode by a bright, orthogonally polarized Floquet-Bloch soliton

Next, we carried out an experiment, in which the waveplate was adjusted such that the beam constituted of a weak TE component and a strong TM one. At high power levels the TM component exhibits nonlinear behavior (practically unaffected by the presence of the weak TE component), creating a localized mode, which traps the weak TE beam. This study extends earlier work done in 2D slab waveguides [18], which demonstrated trapping and guiding of orthogonally polarized femtosecond signals, using bright spatial solitons and a weak signal beam in an AlGaAs planar waveguide.

We launched a mixed-polarization beam into band 2 using the side coupling geometry, and found that it exhibits focusing at a total peak power of 1550 W (Fig. 9(a)). The TM component, carrying a peak power of 1380 W (89% of the total power, see Fig. 9(b)) and the TE component, carrying a peak power of 170 W (11%, Fig. 9(c)) are both focused to about the same width. When launching only the TM component, the beam exhibits self-focusing to the same extent as in (a) (not shown), however the TE component on its own exhibits strong diffraction (Fig. 9(d)). By comparing the TE component of the mixed beam to the fully focused TE beam in Fig. 7 we see that the TE component, which is too weak to self focus, has focused because of the overlapping presence of the self focused TM beam. The high-power TM component created an effective array-defect by self-phase-modulation, and the TE component is guided by this defect. This is in contrary to the vector soliton case, in which both components are needed to create the array-defect, and both make up the composite mode of the induced waveguide [23].

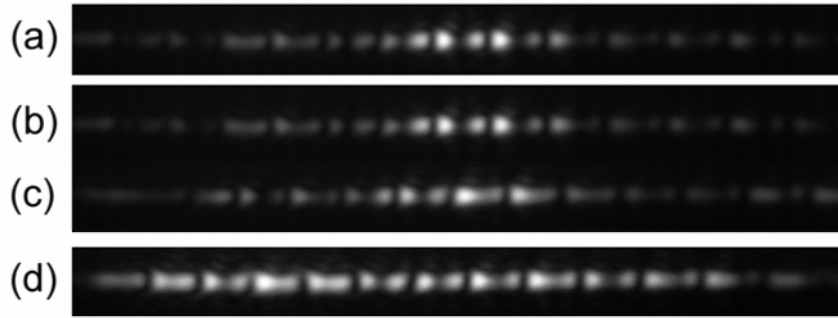


Fig. 9. Guiding of a weak Floquet-Bloch mode by a bright, orthogonally polarized Floquet-Bloch soliton: A beam which consists of a low peak power (170 W) TE component and a high peak power (1380 W) TM component is launched into band 2. When both components are present they exhibit focusing. (a) Shows both components, (b) shows the TM component and (c) the TE component. (d) Shows the TE beam at the same peak power (170 W) without the TM component being present. The presence of a high power TM beam has induced focusing of the weak TE component as well.

The width of the trapped TE component is almost the same as that of the self-trapped, strong, TM component. This is a direct consequence of the near equality between the self phase modulation nonlinearity and the cross phase modulation nonlinearity in AlGaAs, which leads to roughly the same induced index potential for both beams [14].

3.3 Formation and break-up of a multiband breather

The unique situation in which there is virtually no gap in TM between the second and the third bands enabled us to launch a beam in the TM polarization that couples to both the second and the third bands. This was easily achieved as can be seen from the different modal shapes on the left and right in the top panel in Fig. 10(a). Here we investigate the result of an increase in the power coupled into the sample in this situation. We found that as the power increased the beam self-focused until reaching its width at the array input, still maintaining both band components (Fig. 10(a), middle panel). Further increase of the input power resulted in break up of the beam into two components, each residing in a different band (bottom panel in Fig. 10(a)).

A top view of the beam's propagation in the sample (Fig. 10(c)), made possible at high powers due to multiphoton fluorescence at the AlGaAs electronic band gap [24], revealed a clear beating pattern. We verified that the beating is observed only at those angles in which both bands are simultaneously excited. We conclude that the two components belonging to different bands trap together and form a *moving breather* [25].

Breathers are nonlinear localizations [25] characterized by internal oscillations, in contrast to solitons, which maintain a constant shape. Multiband Breathers have been addressed before both experimentally [24] and theoretically [26, 27]. Those breathers were launched in a head-on geometry, exciting simultaneously the first (guided) and second (antiguided) band, but were stationary in the transverse direction. Here we launch a beam composed of two different high, antiguided bands that exhibits self-focusing and beating, while moving in the transverse direction.

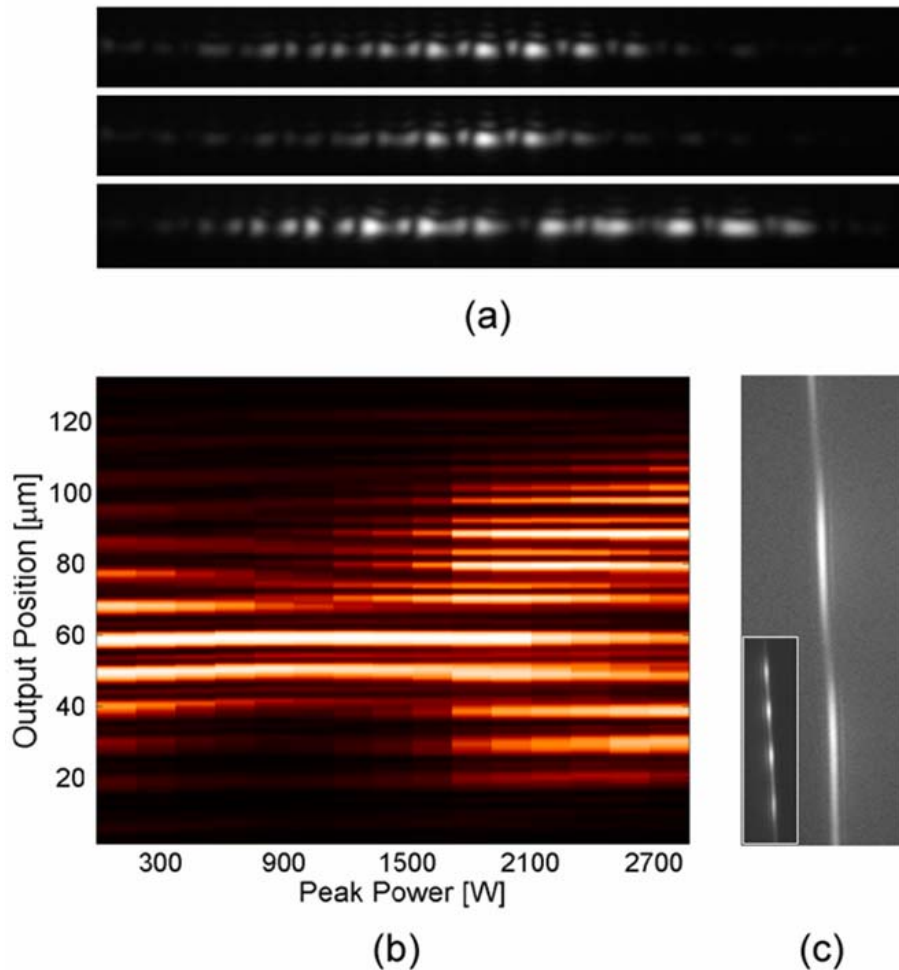


Fig. 10. A multiband moving breather formation and breakup: (a) A view of the array's output facet with the input beam tilted to an angle in which a moving breather is formed at low output power (top), medium (middle) and high power (bottom). The beam is composed of two different bands at all powers, as can be easily seen from the different characteristic modal shapes of the 2nd and 3rd band on the left and on the right. (b) Normalized output intensity distribution at the output facet as a function of output power. Clear focusing of the beam is observed, and then the beam breaks up into two components, each component residing in a different band. (c) Photograph of the waveguide array as seen from above, showing the multiphoton fluorescence emitted by beam, exhibiting a clear beating pattern.

4. Conclusions

We have investigated polarization-dependent effects in nonlinear waveguide arrays. We found that in certain samples the band gap structure is markedly different for the two polarization components, namely, the complete absence of a gap for one polarization, a fact we could not explain by calculations based on the effective index approximation. Clearly, a more precise vectorial calculation is required to explain these observations. Near the missing gap different modal shapes and different band transition angles also characterized the two polarization components. Nonlinear studies demonstrated formation of FB solitons in both polarizations, showing that they maintain their polarization-dependent modal shapes. We also investigated

the nonlinearly induced guiding that a strong beam may inflict on a weak, orthogonal beam via cross phase modulation and observed formation of Vector solitons in high bands. Finally, the absence of the band-2/band-3 gap in the TM polarization has enabled us to demonstrate the formation and breakup of a multiband moving breather.

Acknowledgments

The authors acknowledge financial support from the German-Israeli Project Cooperation (DIP). Y.L. would like to thank A. Buxboim.